Dental Materials Journal 2014; 33(4): 476–483

Three-dimensional X-ray micro-computed tomography analysis of polymerization shrinkage vectors in flowable composite

Yukihiko TAKEMURA[1,2], Koji HANAOKA[3], Ryota KAWAMATA[2], Takashi SAKURAI[2] and Toshio TERANAKA[1]

[1] *Department of Cariology and Restorative Dentistry, Graduate School of Dentistry, Kanagawa Dental University, 82 Inaokacho, Yokosuka, Kanagawa 238-8580, Japan*

[2] *Department of Radiopraxis Science, Graduate School of Dentistry, Kanagawa Dental University, 82 Inaokacho, Yokosuka, Kanagawa 238-8580, Japan*

[3] *Department of Dental Education, Graduate School of Dentistry, Kanagawa Dental University, 82 Inaokacho, Yokosuka, Kanagawa 238-8580, Japan*

Corresponding author, Koji HANAOKA; E-mail: hanaoka@kdu.ac.jp

The polymerization shrinkage of flowable resin composites was evaluated using air bubbles as traceable markers. Three different surface treatments *i.e.* an adhesive silane coupling agent, a separating silane coupling agent, and a combination of both, were applied to standard cavities. Before and after polymerization, X-ray micro-computed tomography images were recorded. Their superimposition and comparison allowed position changes of the markers to be visualized as vectors. The movement of the markers in the resin composite was, therefore, quantitatively evaluated from the tomographic images. Adhesion was found to significantly influence shrinkage patterns. The method used here could be employed to visualize shrinkage vectors and shrinkage volume.

Keywords: Flowable resin composite, Micro-computed tomography, 3D analysis, Polymerization shrinkage, Shrinkage vectors

INTRODUCTION

Flowable resin allows cavities to be treated more easily and with less intervention; it is, therefore, widely used[1)], and there are high expectations for flowable resin composites[2)]. For example, improvements in adhesion and resin adaptation have been reported, and the interface stress of resins during lining relaxation has been reduced[3,4)]. The shrinkage of a resin during polymerization greatly affects the prognosis of a restoration.

Polymerization shrinkage is an unavoidable property of resin restorations. The amount and direction of shrinkage are important factors in cavity adaptation[5)]. Problems such as contraction gaps occur if the shrinkage stress is greater than the adhesion between the resin and the cavity[6,7)], and white margins may occur due to cohesive failure of the enamel wall despite sufficient adhesion[8)]. To avoid these problems, monomers with low shrinkage have been developed[9)], application methods or techniques have been improved[10-12)], and low-energy light-induced polymerization methods have been further improved[13,14)]. The development of such improvements requires basic analytic investigations of the polymerization shrinkage of the resins in cavities.

Light-cured composites are widely considered to show shrinkage oriented toward the irradiated surface of the restoration[3,15)]. However, shrinkage in cavities is mainly influenced by adhesion, flow on the free surface, and local polymerization[5)]. The location and orientation of the irradiating light are also important factors in improving cavity adaptation[16,17)].

Finite-element[18,19)] or photoelasticity[20)] analyses are conventional evaluation techniques used to assess the polymerization shrinkage patterns shown by resins. They are *in silico* modeling studies that use the theoretical characteristics of each composite; therefore, they do not explore the shrinkage behavior of *in vivo* cavities. Cavity adaptation (micro-leakage tests)[21)] can be evaluated using truncation (sectioning) tests after pigmentary infiltration. However, this is a destructive technique, resulting in sample loss. Such tests can only be applied as a partial evaluation on selective areas near the cleavage site[22)]; many samples would be required for full cavity adaptation assessment. The development of imaging techniques such as micro-computed tomography (μCT) allows the non-destructive, three-dimensional study of cavity adaptation in resin restoration and of the orientation of polymerization shrinkage[23)].

The purpose of this study was to examine polymerization shrinkage behavior and cavity adaptation of flowable composite resin three-dimensionally by using a μCT via the measurement of volumetric changes and analysis of shrinkage vectors using air bubbles as markers.

MATERIALS AND METHODS

Materials used

Table 1 lists the resin composite, resin block, and cavity treatment used in this study. As filling materials, nanohybrid-type, A1 shade flowable resin (MI FLOW, (MIF) GC Tokyo, Japan) was used with a uniform filler (700 nm mean particle size) dispersed at high density.

Received Oct 17, 2013: Accepted Mar 20, 2014
doi:10.4012/dmj.2013-288 JOI JST.JSTAGE/dmj/2013-288

Table 1 Materials used

Brand name	Composition	Batch no.	Manufacturer
Nano Hybrid Resin			
MI FLOW	Matrix (31wt%) UDMA Bis-MEPP TEGDMA Photocatalyst Fillers (69wt%) Colloidal Silica Special surface treatment strontium	1001061	GC
Composite block			
GN-I COMPOSITE BLOCK	Urethane-based methacrylate, multifunctional methacrylate, silica nanofillers, fine particle glass fillers (average 1.0 μm) prepolymerized fillers, photoinitiator, pigments	1003251	GC
Surface modifier			
RelyX™ Ceramic Primer	3-methacryloxypropyltrimethoxysilane Ethanol Water	N208566	3M ESPE
10F2S-3I	1H,1H,2H,2H-henicosafluorododecyltriisocyanatosilane [$F(CF_2)_{10}(CH_2)_2Si(NCO)_3$] Hydrofluoroether		Tokyo University of Science

Model cavity blocks (GN-1, GC, Tokyo, Japan, shade A1) were made by polymerizing MFR-type resin at high temperature and pressure. Cavity treatment employed either or both of an adhesive silane coupling agent (RelyX™ Ceramic Primer, 3M ESPE, Dental Products, St Paul, USA) and a separating silane coupling agent with a long fluorocarbon chain and marked water- and oil-repellency properties, 1H, 1H,2H,2H-henicosafluorododecyltriisocyanatosilane (10F2S-3I, $F(CF_2)_{10}(CH_2)_2Si(NCO)_3$). 10F2S-3I was developed as a tooth-modifying separating agent with plaque adhesion resistance[24-27].

Measurement methods

Figure 1 shows a schematic of the sequence followed in this experiment. A dental CAD/CAM system (GM1000, GC, Tokyo, Japan) was used to make cylindrical standard cavities (4 mm inner diameter, 2.4 mm depth, and 3.4 C-factor) in resin blocks. Each cavity was immersed in 1 mol/L sodium hydroxide solution, cleaned in an ultrasonic cleaner for 5 min, cleaned with acetone, and then dried. The dependence of shrinkage behavior on the adhesion between the cavity and the resin composite was investigated using three kinds of cavity treatments. Group A cavities had the adhesive silane coupling agent applied over the whole cavity to provide adherence between the whole cavity and the resin composite. Group B cavities were completely coated with the separating silane coupling agent to minimize adherence between the whole cavity and the resin composite (*i.e.,* to exclude binding forces). Group C samples had the adhesive agent applied on the side wall of the cavity, and the separating agent applied on the cavity floor to simulate the results of recent adhesive tests[7,28,29]: the adhesive agent on the side wall —which in a tooth includes the mainly mineral enamel— polymerized early and adhered well. The separating agent at the cavity floor —which in a tooth consists of dentine, including many organic matters— polymerized slowly owing to its distance from the light source and adhered poorly. Under safe lighting, the flowable resin was mixed by hand for 30 s to incorporate air bubbles; it was then filled into the cavities using a constant-rate syringe without any adhesive application. Images were then immediately recorded by μCT (MCT-CB100MF, Hitachi Medical Corporation, Tokyo, Japan; 80 kV tube voltage, 100 μA tube current, ×10 magnification). The μCT device emitted light from 1 mm above the samples for 40 s. Further μCT images were recorded after polymerization induced by radiation from a 5.5 mm diameter, 700 mW/cm^2 halogen lamp (JET Light 3000, J. Morita Co., CA , USA).

Superimposition of the two sets of μCT images allowed identification of the changes induced by polymerization. The shrinkage on the free surface and the formation of gaps on the side wall and cavity floor were quantitatively determined. The data were analyzed using the Turkey-Kramer test with a 95% confidence interval to indicate significant difference among the groups. An air-bubble-centered coordination system was

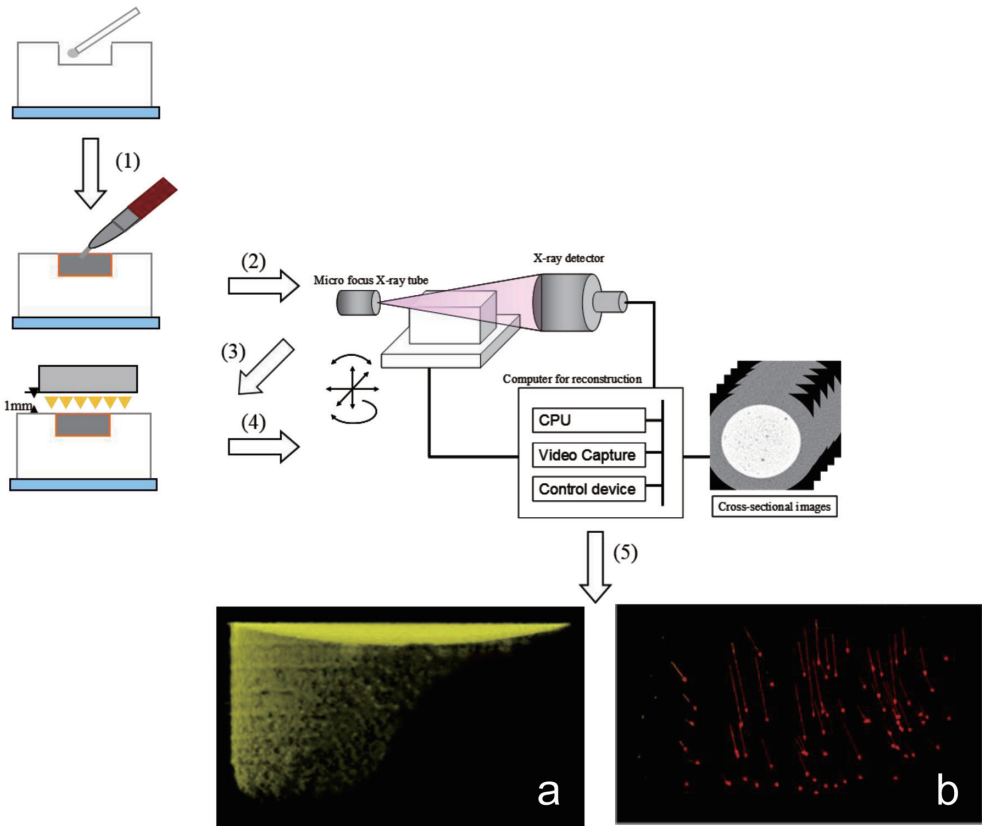

Fig. 1 Measurement of polymerization shrinkage with resin flow.
(1) Adhesive or separating silane coupling agents are applied to the cavity, which is then filled with flowable resin mixed to incorporate air bubbles. (2) μCT images are immediately captured. (3) Photopolymerization is performed for 40 s. (4) μCT images are again immediately captured. (5) Images before and after the polymerization are superimposed to show (a) shrinkage on the free surface and gap formation in the cavity, and (b) the internal movement of air bubbles in the resin. Group C: The figure on the right representative example a partial gap formation of the side walls. The left figure shows a typical example overall gap formation of the side walls.

established, and positional changes were visualized as vectors. Then, the internal flow in the resin composite was quantitatively evaluated using X-ray μCT with air bubbles used as markers. Air bubbles of 50–110 μm were identified in the data recorded before polymerization. Unevenly dispersed bubbles and those larger than 110 μm were excluded. The relationship between the vertical position of each marker and its movement (*i.e.,* its positional change) was evaluated in detail via regression analysis using least squares.

Effect of cavity treatments with RelyX Ceramic Primer and 10F2S-3I on bond strength was enables. Finely polished GN-1 with 600-grit SiC paper under continuous running water were used as adherents. All GN-1 blocks were cleaned and dried by previous mentioned procedure.

Masking tape with a 2 mm diameter hole was placed on the GN-1 surface, and a Teflon tube with a 2.38 mm internal diameter was positioned in the hole. After RelyX Ceramic Primer and 10F2S-3I were applied onto the surface for 30 s, MIF was filled to a height of approximately 2 mm in the tubes and illuminated for 40 s from the top surface of the resin composite with the visible light-curing unit. After the resin composite was cured, the tubes and tapes were removed.

Micro shear bond test was performed on a universal testing machine (Ez-test-500N, SHIMAZU Corporations, Kyoto, Japan) at a cross head speed of 1 mm/min with an apparatus reported previously. A thin wire (diameter 0.20 mm) was looped around the resin cylinder, making contact through half its circumference, and was gently held flush against the MIF/GN-1 interface. The mean shear bond strength was calculated from results of 8 specimens. As control, shear bond strength of MIF/untreated GN-1 was measured.

RESULTS

Changes in outer form and vectors

The extracted images (Fig. 2) reveal shrinkage on the free surface and gap formation on the side wall and the cavity floor. Polymerization shrinkage vectors, which mark the changes, are also shown in the figure.

Group A exhibited a marked recess of resin composite at the center of the free surface. All samples showed some detachment from the side wall, with wider detachment closer to the surface. However, Group A showed no gaps on the cavity floor. Some of the samples showed collar-shaped gaps of approximately 100 μm. Most of the markers were displaced diagonally downwards towards the side wall that had maintained adhesion and towards the cavity floor (*i.e.*, the vectors were generally oriented to a point at the edge of the cavity floor). Movement was greater in areas closer to the free surface and less in areas closer to the cavity floor.

Group B showed fewer external changes on the free surface than did Group A. Similar to Group A, one side exhibited greater shrinkage. Gaps appeared around almost the entire circumference of the side wall of the cavity. Only small gaps appeared on the cavity floor, and the movement of the markers was greatest at the surface. Some vectors were oriented toward the center of the cavity floor, while others were oriented toward the side wall or toward the edge of the cavity floor. The orientations are somewhat irregular: on the cavity floor, the markers had moved in many directions.

Group C showed distinctive shrinkage on the free surface and the cavity floor. On the side wall, three of six samples did not exhibit detachment but did show clear gap formation on the cavity floor, differing from groups A and B. Some samples that maintained good adherence to the side walls showed vectors that were oriented downward near the free surface and upward near the cavity floor; *i.e.*, the vectors were oriented toward the central horizontal plane (if not the center specifically) of the cavity. Few vectors were oriented toward the side wall when adhesion was maintained. In some samples that showed partial detachment on the side wall, the markers had moved diagonally and downward, toward the areas of the side wall that maintained adhesion. Some other samples also showed movement near the free surface. Near the cavity floor, diagonally upward movement was directed toward the area of the side wall that maintained adhesion. On the side wall, the markers were displaced from the areas of detachment toward the areas of the side wall that maintained adhesion. The latter movement matched the orientation of the outer changes.

Shrinkage and gap formation during polymerization

Table 2 lists the average volume of shrinkage on the free surface and the gap formation on the side walls and on the cavity floors shown by typical samples.

Group A showed significantly greater shrinkage on the free surface than did groups B or C ($p<0.05$). Group B showed significantly greater gap formation on the side wall than did other groups ($p<0.05$). Group C showed significantly greater gap formation on the cavity floor than did groups A or B ($p<0.05$). However, there was no significant difference between the total shrinkage shown by the three groups.

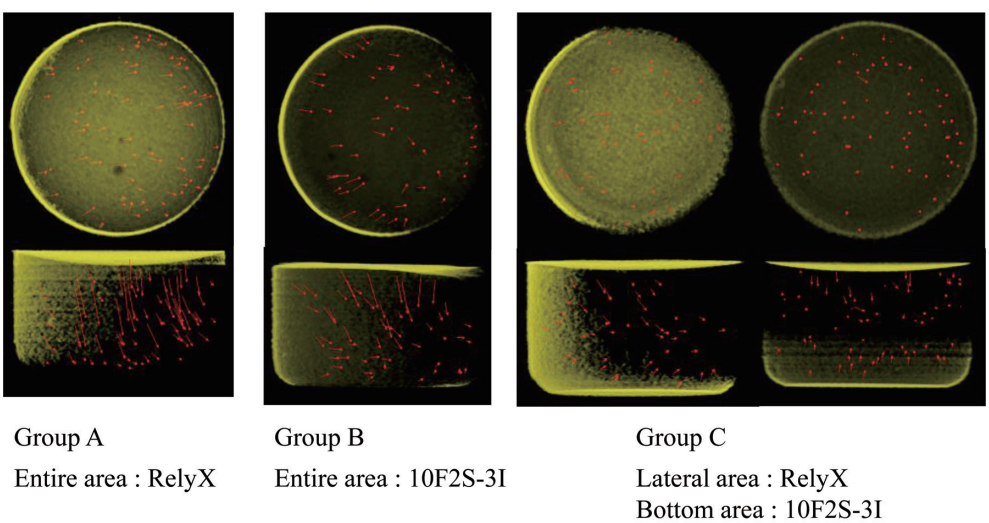

Fig. 2 Polymerization shrinkage and shrinkage vectors.
Upper figures show the top surfaces and lower figures show side views of typical samples from each group. Outer changes on the free surface and gap formation due to polymerization are shown in yellow. Position changes of the bubbles before and after polymerization are decoupled to depict the vectors at 10× magnification.

Table 2 Percentage volume changes of interfacial gap and shrinkage volume fraction (mean and S.D., n=6, pooled values)

(volume%)	Group A	Group B	Group C
Free surface contraction	3.96±0.06 [a]	2.67±0.25 [b]	2.20±0.53 [b]
Side wall contraction	0.89±0.06 [a]	2.19±0.16 [b]	1.16±0.07 [c]
Cavity floor contraction	0.00±0.01 [a]	0.14±0.04 [a]	1.65±0.27 [b]
Total contraction	4.87±0.08 [a]	4.99±0.12 [a]	5.01±0.46 [a]

Tukey-Kramer test was conducted to compare the three groups.
Each letter label (a, b, and c) denotes sets of mean values with no statistically significant differences (p>0.05).

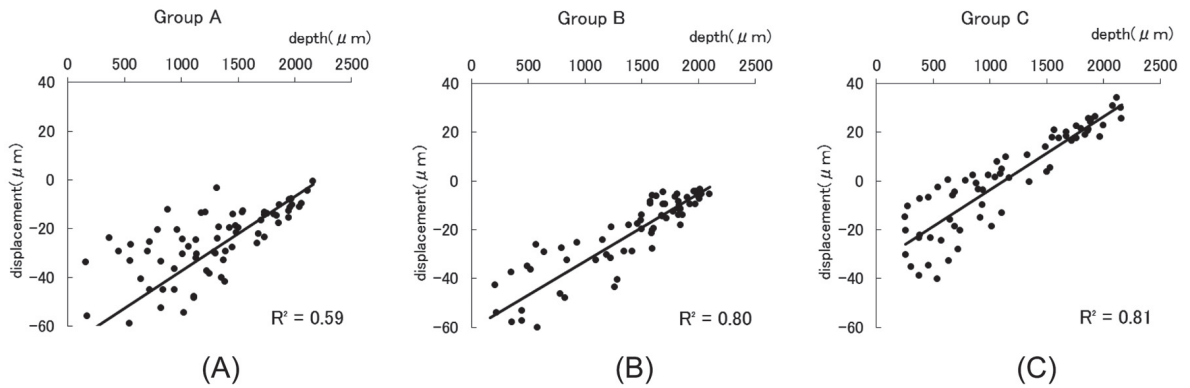

Fig. 3 Relationship between depth and movement of marker bubbles.
Results show vertical movements of markers in typical samples in the three groups. On the y-axis, a positive value denotes movement toward the free surface; a negative value, toward the cavity floor. The x-axis denotes the distance from the upper margin of the standard cavity (*i.e.*, the free surface).
Groups A and B showed large downward movements near the free surface and smaller downwards movements at sites located farther from the free surface.
Group C samples showed downward movements in their upper halves and upward movements in their deeper halves.

Table 3 Effect of cavity treatments on bond strength (mean and S.D., n=8)

	Untreatment	RelayX	10F2S-3I
Bond strength (MPa)	6.4±1.3	17.3±3.5	0.4±0.1

Tensile shear bond strengths test were analyzed using one-way analysis of variance (ANOVA) with a 95% confidence interval to indicate significant differences.
Significant differences were found among three groups. (p<0.05).

Relationship between depth and movement of air bubbles (vertical relationship)
Figure 3 illustrates typical relationships between the vertical positions of the markers, (*i.e.*, their depth) and their vertical movement in each of the three groups. Groups A and B both showed movement only toward the cavity floor (*i.e.*, the negative direction in Fig. 3); the magnitude of the movement was greatest closest to the free surface. However, Group B showed less dispersion than did Group A, and it showed a high correlation between depth and movement of marker bubbles (R^2=0.80). Group C showed movement in both vertical directions: movement was in the negative direction near the free surface, and near the cavity floor the bubbles moved upward. The movements were collectively toward the central horizontal plane of the cavity. The positions of the air bubbles and their vertical movement were highly correlated (R^2=0.81).

Tensile shear test
The measured bond strength are shown in Table 3. An ANOVA showed significant differences in mean bond

strength among three treatment groups($p<0.05$). While the use of RelyX Ceramic Primer effectively raised the bond strength value, 10F2S-3I solution significantly reduced the value.

DISCUSSION

Several μCT studies have been conducted on the polymerization shrinkage of light-cured composite resins[21,23,30-32]. Some aimed to express the shrinkage behavior as three-dimensional vectors by adding markers to the resin composite and analyzing their movement[30-32].

Zirconia fillers[23] have been used as markers. However, the addition of such markers may have influenced the viscosity of the resin composite, thus affecting its shrinkage behavior. The specific gravity of the markers, the presence or absence of surface treatments, and their dispersion method could each affect the shrinkage of a resin. Zirconia fillers, while being useful detecting markers, can relax internal stress, disturbing adhesion to the resin composite[35,36]. The incorporation of markers complicates and increases the cost of assessment.

In this experiment, air bubble was selected as traceable marker. In general, it is estimated that oxide in air bubbles may prevent the polymerization of composite resin and relax the internal stress of a resin composite. However, we believe that this proposed simple method using air bubbles is effective method that allow the evaluation of three-dimensional shrinkage without resin's compositional change.

A method of mixing air bubbles into the resin was developed to control their size and volume; therefore, bubbles of similar sizes could be consistently mixed. Only bubbles of 50–110 μm were considered in the analysis for uniformity. A GN-1 resin block was used as a standard cavity. The resin block had a CT value of 522.3±27.2, approximately one tenth of that shown by the flowable resin (5,649.6±176.6). The bolder site could clearly be detected when the minute gaps were measured using μCT.

The free surface was consistently displaced toward the cavity floor in each of the three groups. Displacement was greatest at the center, because the flowable resin had sufficient flow, and an unpolymerized layer may have been produced owing to it being exposed to the atmosphere. The flow orientation in the resin composite matched the observed exterior changes. Each of the three groups exhibited different adhesion behaviors and different flow orientations around the side walls and cavity floors.

A large hollow in the center of the free surface was observed in Group A. This might have been caused by a flow of the resin composite to compensate contraction stress, because much of the side wall and the cavity floor remained adhered. This effective adhesion was attributed to RelyX Ceramic Primer that increased shear bond strength between GN-1 composite block and MIF (Table 3). The shrinkage vectors were oriented toward the adhesion sites. This suggests that adhesion might have been important in determining the flow of the resin composite and the shrinkage orientation. The significantly greater gap formation on the side wall shown by Group B may have arisen because chemical adhesion was not achieved anywhere in the cavity. This results indicated that 10F2S-3I acted as separating agent (Table 3). This likely resulted in stress not being concentrated on the free surface and the orientation of shrinkage showed no distinct pattern. Group C maintained the best adhesion to the side wall, leading to polymerization shrinkage being compensated by movement at both the free surface and the cavity floor.

Around the cavity side wall at the surface, detachment and adhesion sites occurred symmetrically in groups A and C. Despite the similar adhesion conditions, evenly distributed adhesion to the side walls was difficult to achieve. Slight differences, such as the reaction to the silane coupling agent or the starting point of polymerization, may have resulted in significant differences that led to only one side adhering. Detachment was greatest at the top of the cavity and attenuated with increasing depth. Polymerization may have started sooner at the top surface because it was closer to the light source, leading to greater shrinkage[34]. The cavity size used here and the selected C-factor of 3.4 might also have influenced the development of shrinkage[35,36].

Regarding the shrinkage pattern observed in Group B, it is estimated that contact was maintained between the resin composite and the cavity, and that changes in the position of resin on the side wall were minimal, as the 10 nm 10F2S-3I tri-molecular layer[24] allows the resin composite to interlock with the separating silane coupling agent. However, group B showed greater gap formation on the side wall, possibly due to free shrinkage toward the center of the resin mass and the side wall, as the large surface area compensates for shrinkage stress. Given that gaps formed at the side wall but not at the cavity floor, the whole resin composite in the cavity may have moved down.

Unlike Groups A and B, Group C showed clear gaps on the cavity floor where 10F2S-3I had been applied. The shrinkage at the cavity floor relaxed the shrinkage stress in the rest of the resin composite, allowing effective adhesion to be maintained on the side wall. The light-polymerizable flowable resin shrunk consistently toward the center of the sample, even in the parts not oriented toward the radiation source.

No statistically significant differences were observed for total shrinkage between the three groups. Under the conditions of this study, polymerization shrinkage was manifested as outer changes of the free surface and as detachment from the cavity wall and floor in areas of inferior adhesion. The internal flow of the resin composite was oriented toward the areas that maintained adhesion. Volumetric shrinkage may generate and maintain a large contraction stress within a restored cavity in cases that show no interface gap formation.

Flowable resin appeared effective as an adhesive restoration material due to its characteristics such as improved wettability, adhesion and its flowability or stress-relaxation at the adhesive interface. However, large polymerization shrinkage could increase the risk of detachment within the cavity, which may cause microleakage, post-operative sensitivity, and secondary caries.

The present study is the first to clarify the adhesion of resin to the cavity and the relationship between exterior changes of the flowable resin and its internal flow. We showed that multi-layered filling is required through an analysis of shrinkage orientation, and developed a method of assessing polymerization shrinkage for clinical use.

CONCLUSIONS

Shrinkage patterns are strongly influenced by adhesion of cavity, and the use of μCT images with air bubbles as trace makers can visualize shrinkage vectors and shrinkage volume.

These results conflict with previous findings that the shrinkage vector of light-cured composites is oriented toward the irradiated surface of the restoration.

ACKNOWLEDGMENTS

This work was supported, in part, by a Grant-in-Aid for Scientific Research (C) (24592887) from the Japan Society for the Promotion of Science (JSPS).

REFERENCES

1) Tyas MJ, Anusavice KJ, Frencken JE, Mount GJ. Minimal intervention dentistry-a review. FDI Commission Project 1-97. Int Dent J 2000; 50: 1-12.
2) Wattanawongpitak N, Yoshikawa T, Burrow MF, Tagami J. The effect of bonding system and composite type on adaptation of different C-factor restorations. Dent Mater J 2006; 25: 45-50.
3) Versluis A, Tantbirojn D, Douglas WH. Do dental composites always shrink toward the light? J Dent Res 1998; 77: 1435-1445.
4) Kato H. Relationship between the velocity of polymerization and adaptation to dentin cavity wall of light-cured composite. Dent Mater J 1987; 6: 32-37.
5) Asmussen E, Jorgensen KD. A microscopic investigation of the adaptation of some plastic filling materials to dental cavity walls. Acta Odontol Scand 1972; 30: 3-21.
6) Ferracane JL, Mitchem JC. Relationship between composite contraction stress and leakage in Class V cavities. Am J Dent 2003; 16: 239-243.
7) Condon JR, Ferracane JL. Reduced polymerization stress through non-bonded nanofiller particles. Biomaterials 2002; 23: 3807-3815.
8) Jörgensen KD, Asmussen E, Shimokobe H. Enamel damages caused by contracting restorative resins. Scand J Dent Res 1975; 83: 120-122.
9) Papadogiannis D, Kakaboura A, Palaghias G, Eliades G. Setting characteristics and cavity adaptation of low-shrinking resin composites. Dent Mater 2009; 25: 1509-1516.
10) Winkler MM, Katona TR, Paydar NH.Finite element stress analysis of three filling techniques for class V light-cured composite restorations. J Dent Res 1996; 75: 1477-1483.
11) Versluis A, Douglas WH, Cross M, Sakaguchi RL. Does an incremental filling technique reduce polymerization shrinkage stresses? J Dent Res 1996; 75: 871-878.
12) Akutagawa T. A study on the apical marginal adaptation of composite restoration. Jpn J Conserv Dent 1993; 36: 1-12.
13) Yoshikawa T, Burrow MF, Tagami J. A light curing method for improving marginal sealing and cavity wall adaptation of resin composite restorations. Dent Mater 2001; 17: 359-366.
14) Kanca J 3rd, Suh BI. Pulse activation: reducing resin-based composite contraction stresses at the enamel cavosurface margins. Am J Dent 1999; 12: 107-112.
15) Asmussen E, Peutzfeldt A. Direction of shrinkage of light-curing resin composites. Acta Odontol Scand 1999; 57: 310-315.
16) Hansen EK. Visible light-cured composite resins: polymerization contraction, contraction pattern and hygroscopic expansion. Scand J Dent Res 1982; 90: 329-335.
17) Lutz F, Krejci I, Luescher B, Oldenburg TR. Improved proximal margin adaptation of Class II composite resin restorations by use of light-reflecting wedges. Quintessence Int 1986; 17: 659-664.
18) Roulet JF, Salchow B, Wald M. Margin analysis of posterior composites in vivo. Dent Mater 1991; 7: 44-49.
19) Winkler MM, Chen J, Qian H, Hamula DW, Carlson TJ, Katona TR. Experimental validation of a finite element model of light-activated polymerization shrinkage. J Biomed Mater Res 2000; 53: 554-559.
20) Johnson EW, Castaldi CR, Gau DJ, Wysocki GP. Stress pattern variations in operatively prepared human teeth, studied by three-dimensional photoelasticity. J Dent Res 1968; 47: 548-558.
21) Sun J, Eidelman N, Lin-Gibson S. 3D mapping of polymerization shrinkage using X-ray micro-computed tomography to predict microleakage. Dent Mater 2009; 25: 314-320.
22) Tay FR, Pashley DH, Yiu C, Cheong C, Hashimoto M, Itou K, Yoshiyama M, King NM. Nanoleakage types and potential implications: evidence from unfilled and filled adhesives with the same resin composition. Am J Dent 2004; 17: 182-190.
23) Cho E, Sadr A, Inai N, Tagami J. Evaluation of resin composite polymerization by three dimensional micro-CT imaging and nanoindentation. Dent Mater 2011; 27: 1070-1078.
24) Yoshino N, Yamamoto Y, Teranaka T. Surface modification of denture to provide contamination-free ability by using silane coupling agent containing fluorocarbon chain. Chem Lett 1993; 22: 821-824.
25) Teranaka T, Iwamoto T, Yoshino N. Application of newly developed surface modifier to dental material. Bull Kanagawa Dent Coll 1994; 22: 151-155.
26) Yoshino N, Teranaka T. Synthesis of silane coupling agents containing fluorocarbon chain and applications to dentistry: plaque-controlling surface modifiers. J Biomater Sci Polymer Ed 1997; 8: 623-653.
27) Yoshino N, Yamauchi T, Kondo Y, Kawase T, Teranaka T. Plaque-controlling surface modifier containing fluorocarbon chain. React Funct Polym 1998; 37: 271-282.
28) Yahagi C, Takagaki T, Sadr A, Ikeda M, Nikaido T, Tagami J. Effect of lining with a flowable composite on internal adaptation of direct composite restorations using all-in-one adhesive systems. Dent Mater 2012; 31: 481-488.
29) Bista B, Sadr A, Nazari A, Shimada Y, Sumi Y, Tagami J. Nondestructive assessment of current one-step self-etch dental adhesives using optical coherence tomography. J Biomed Opt 2013; 18: 76020.
30) Chiang YC, Rosch P, Dabanoglu A, Lin CP, Hickel R, Kunzelmann KH. Polymerization composite shrinkage evaluation with 3D deformation analysis from microCT images. Dent Mater 2010; 26: 223-231.

31) Sun J, Lin-Gibson S. X-ray microcomputed tomography for measuring polymerization shrinkage of polymeric dental composites.Dent Mater 2008; 24: 228-234.
32) Kakaboura A, Rahiotis C, Watts D, Silikas N, Eliades G. 3D-marginal adaptation versus setting shrinkage in light-cured microhybrid resin composites. Dent Mater 2007; 23: 272-278.
33) Feng L, Suh BI, Shortall AC. Formation of gaps at the filler-resin interface induced by polymerization contraction stress: Gaps at the interface. Dent Mater 2010; 26: 719-729.
34) Feilzer AJ, de Gee AJ, Davidson CL. Setting stresses in composites for two different curing modes. Dent Mater 1993; 9: 2-5.
35) Yoshikawa T, Sano H, Burrow MF, Tagami J, Pashley DH. Effects of dentin depth and cavity configuration on bond strength. J Dent Res 1999; 78: 898-905.
36) Yoshikawa T, Wattanawongpitak N, Tagami J. Effect of C-factor on bond strength to cavity wall. Jpn J Conserv Dent 2011; 54: 20-25.